


## RESEARCH ARTICLE

# Conservation Tillage Increases Carbon Storage by Regulating Mineral-Mediated Aggregate Stability and Carbon Chemistry

Zixuan Han<sup>1,2</sup> | Aurore Degré<sup>2</sup> | Shengping Li<sup>1</sup>  | Xiaojun Song<sup>3</sup> | Huizhou Gao<sup>1</sup> | Angyuan Jia<sup>1</sup> | Qiqi Gao<sup>1</sup> | Xueping Wu<sup>1</sup>  | Aizhen Liang<sup>4</sup>

<sup>1</sup>State Key Laboratory of Efficient Utilization of Arid and Semi-Arid Arable Land in Northern China (The Institute of Agricultural Resources and Regional Planning, Chinese Academy of Agricultural Sciences), Beijing, China | <sup>2</sup>Terra Research Center, University of Liege, GxABT, Gembloux, Belgium | <sup>3</sup>Institute of Agricultural Resources and Environment, Xinjiang Academy of Agricultural Sciences, Ürümqi, China | <sup>4</sup>Northeast Institute of Geography and Agroecology, Chinese Academy of Sciences, Changchun, China

**Correspondence:** Xueping Wu ([wuxueping@caas.cn](mailto:wuxueping@caas.cn)) | Aizhen Liang ([liangaizhen@iga.ac.cn](mailto:liangaizhen@iga.ac.cn))

**Received:** 12 May 2025 | **Revised:** 28 September 2025 | **Accepted:** 27 October 2025

**Funding:** This work was supported by National Key Research and Development Program of China (2023YFD1500301).

**Keywords:** aggregates | carbon functional groups | conservation tillage | minerals | soil organic carbon

## ABSTRACT

Widespread adoption of conservation practices is increasingly encouraged to improve soil organic carbon (SOC) storage and mitigate climate change. However, soil texture and mineralogy cause variable SOC responses under conservation tillage. The role of minerals and organic carbon composition in soil aggregation and SOC stabilization remains insufficiently understood. This study evaluated the long-term effects of conservation tillage (no-tillage with straw return, NTS) versus conventional tillage (plough tillage with straw removal, CT) on carbon storage across Phaeozems, Calcaric Cambisols, and Calcic Luvisols. Compared to CT, NTS increased the annual average C sequestration rate by 15.3%–76.7% and SOC storage by 10.2%–28.4% in different soil types. NTS also increased macroaggregate percentage and mean weight diameter (MWD), resulting in 17.8%–28.3% larger macroaggregate-associated SOC and total nitrogen (TN) contents. Notably, the aromatic-C/aliphatic-C ratio under NTS increased in bulk soil and macroaggregates, which were positively correlated with larger amorphous iron (Feo) content, Ca<sup>2+</sup> concentration, and specific surface area in different treatments. Phaeozems exhibit the largest SOC storage, along with larger Feo and Ca<sup>2+</sup> contents and aromatic-C/aliphatic-C ratio. However, NTS led to the greatest increases in MWD and SOC storage in Calcaric Cambisols, and the greatest enhancement of microbial biomass carbon in Calcic Luvisols. PLS-PM analysis indicated that although the aromatic-C/aliphatic ratio directly enhances aggregated stability, Feo and Ca<sup>2+</sup> promoted MWD indirectly by facilitating greater aromatic-C and polysaccharide-C. Overall, conservation tillage promoted selective binding of Feo and Ca<sup>2+</sup> to SOC functional groups, thus enhancing soil aggregation and SOC physico-chemical protection, with calcareous soils showing a stronger response.

## 1 | Introduction

As the largest carbon reservoir in terrestrial ecosystems, soil organic carbon (SOC) plays a vital role in maintaining soil fertility, ensuring food security, and supporting the sustainability of global agricultural systems (Andruschkewitsch et al. 2013).

However, SOC stocks are increasingly depleted due to intensive agricultural practices, particularly under the pressures of global climate change (Sarker et al. 2018). The stabilization of SOC mainly involves molecular resistance, the adsorption and encapsulation of clay minerals and physical protection from microbial decomposition by soil aggregates (Nandan et al. 2019).

## Summary

- No tillage and straw return (NTS) promoted soil aggregation and mineral-organic associations to increase soil organic carbon (SOC) storage across different soil types.
- Greater amorphous iron (Feo), exchangeable  $\text{Ca}^{2+}$  and aromatic-C/aliphatic-C ratio contributed to aggregate stability under NTS.
- Feo and  $\text{Ca}^{2+}$  correlated positively with aromatic-C but negatively with carboxy-C.
- Phaeozems stored more SOC due to higher Feo,  $\text{Ca}^{2+}$  availability and large macroaggregate proportions.

Consequently, the adoption of sustainable agronomic practices is essential for preserving soil function and quality. A comprehensive understanding of the chemical association of SOC and the protective role of soil aggregates is critical for enhancing soil quality.

It is known that conventional intensive tillage (CT) destroys soil physical structure, leading to SOC mineralization and nutrient loss (Jat et al. 2019). On the contrary, conservation tillage including reduced or no-till and straw return reduces soil disturbance and helps maintain aggregate stability and function (Panettieri et al. 2014). The physical protection provided by soil aggregates is a critical mechanism for SOC storage (Six et al. 2004). Large aggregates physically encapsulate SOC, isolating it from microbial access and protecting it from decomposition (Karlen et al. 2013). The formation of soil aggregates relies on organic binders, like plant and microbial residues, along with inorganic agents including polyvalent mineral ions (e.g.,  $\text{Fe}^{3+}$ ,  $\text{Ca}^{2+}$ ,  $\text{Mg}^{2+}$ ) and clay particles (Xue et al. 2019). No-tillage combined with straw return enhances organic matter inputs and stimulates microbial activity, thereby supplying abundant organic binding agents that facilitate soil aggregate formation (Kan et al. 2020). However, the process of aggregate formation governed by tillage practices depends on the soil environment, and mineral type of the soil. Some soils containing specific minerals, such as red soils with high levels of iron and aluminum oxides, enhance the binding between iron ions and small-molecule organic functional groups (Tivet et al. 2013). Calcium-rich soils can alter the stability of organic carbon by mediating the interaction and binding between calcium ions and microbial decomposition products (Atere et al. 2020). In addition, soil mineral ions can selectively absorb the additional organic matter introduced by straw to form mineral-organic complexes that can act as organic or inorganic binders to agglomerate soil particles (Maltoni et al. 2017). Long-term penetration of straw degradation products into the deep soil can improve the efficiency of straw conversion and offset short-term negative effects (Karlen et al. 2013). Therefore, the effect of long-term no tillage and straw return (NTS) on aggregate formation and SOC sequestration on yield performance in different temperate regions still requires comparative studies.

Different carbon compounds are persistent organic cementing agents that positively influence the formation and stabilization of soil aggregates. The functional groups on the surface of

the aromatic compounds of the soil organic matter cement soil particles together and form stable aggregate structures (Plaza et al. 2013; Sowers et al. 2018). Straw return has been reported to enhance the stability of humic acid by increasing the proportions of O-alkyl C and aromatic-C within the humic acid fraction (Ndzelu et al. 2023). Moreover, organic material addition reduces the degree of condensation and oxidation of aromatic composition, increases the proportion of alkyl-C, and enhances hydrophobicity structures (Li et al. 2022). No tillage increases the proportion of phenols, quinones, aliphatic-C, and hydrophobic-C in the soil and promotes soil aggregation and carbon stability (Xue et al. 2019). More importantly, minerals are also known to bind with the organic carbon functional groups selectively. The less crystalline ferrihydrite with a higher specific surface area (SSA) absorbs more aromatic compounds (Kirsten et al. 2021). In farmlands with long-term organic fertilization and appropriate chemical management, exchangeable Ca ions and carboxyl and aromatic carbon compounds showed positive correlations (Wan et al. 2021). The straw returning also increased the methoxy-C derived from lignin fractions and consequently acts as a hydrophobic material, promoting soil aggregation and carbon stability (Plaza et al. 2013; Urbanek et al. 2007). However, knowledge about the effect of mineral-mediated binding of different carbon functional groups with soil aggregates and their interaction effect on SOC sequestration under conservation tillage in various soil types remains elusive.

Long-term conservation tillage has been shown to maintain soil carbon and nitrogen balance, enhance nutrient availability and soil function (L. Gao et al. 2017; Y. Liang et al. 2021). However, most previous studies have focused on SOC storage at single sites, with limited attention to how variations in mineral composition influence SOC dynamics and interact with carbon functional groups and soil aggregation across different tillage practices and soil types. Based on long-term tillage experiments conducted at three distinct sites, this study aims to: (1) assess the effects of conservation tillage on SOC storage and spatial variability; (2) elucidate the regulatory roles of minerals and organic carbon functional groups in aggregate stability across contrasting soil types; and (3) identify the mechanisms underlying the physical and chemical stabilization of SOC under conservation tillage. We hypothesize that no-tillage combined with straw return enhances mineral ion availability across diverse soil types, thereby facilitating organo-mineral associations through interactions with organic carbon functional groups. These associations are critical for aggregate formation, ultimately improving soil structural stability and influencing long-term carbon sequestration.

## 2 | Materials and Methods

### 2.1 | Experimental Design

This study was carried out on three long-term conservation fields: Changchun (CC, 44°00'N, 125°24' E, Jilin Province), Luoyang (LY, 34.80°N, 112.55°E, Henan Province) and Linfen (LF, 36.01°N, 111.37°E, Shanxi Province), which are located in the semihumid regions of China and exhibit distinct tillage practices (Figure 1). According to the Food and Agriculture

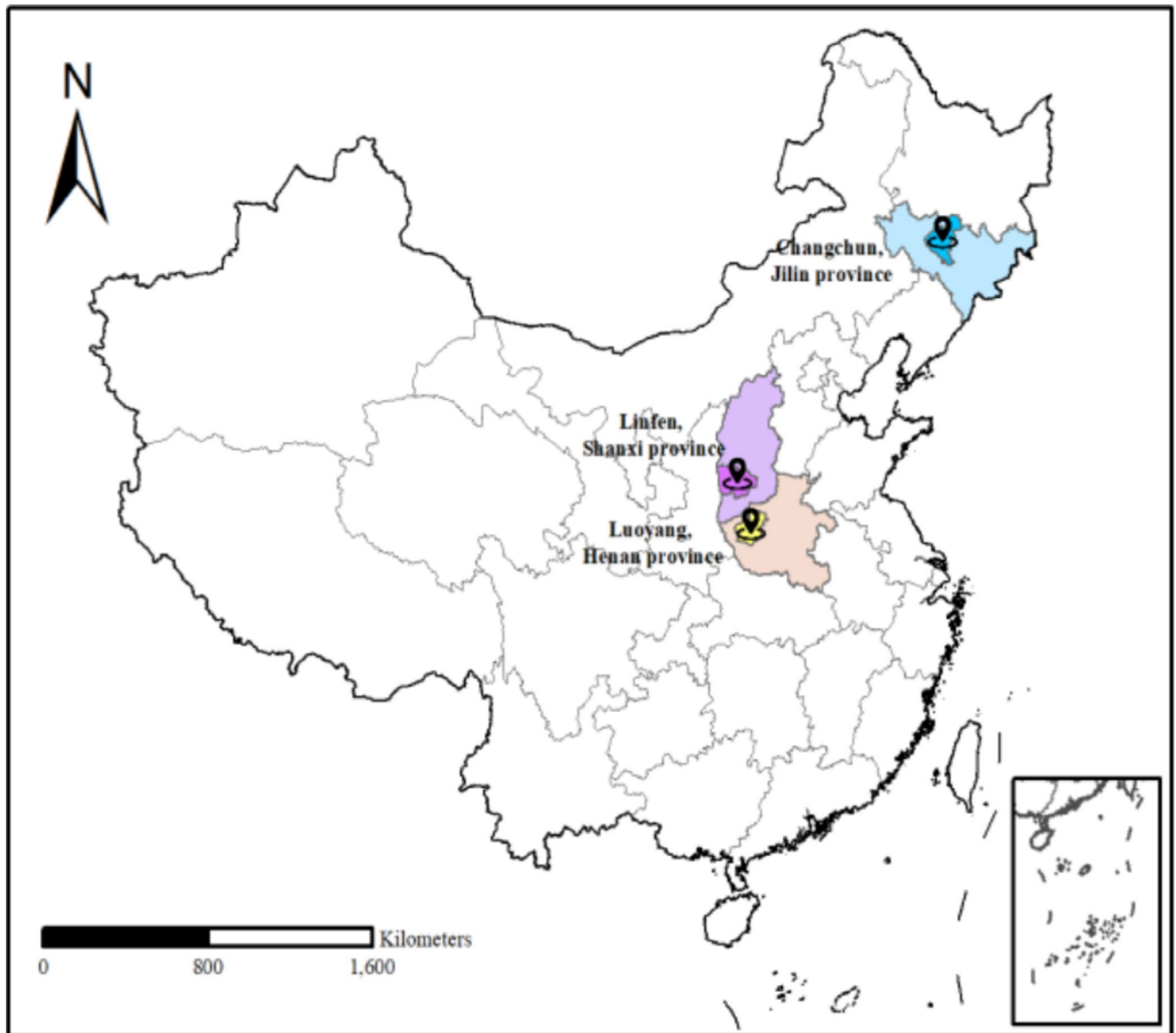


**FIGURE 1** | Location of the study area and sampling sites.

Organization (World Reference Base for Soil Resources 2014 2015), the studied soil in these areas is classified as Phaeozems (CC, Clayic), Calcaric Cambisols (LY, Sandy) and Calcic Luvisols (LF, Siltic) with different particle size distributions (Table 1). These areas belong to a temperate continental monsoon climate that is characterized by an average annual precipitation of between 555 and 650 mm and an average annual temperature of between 4.4°C and 13.7°C (Table 1). Each site is subject to a single season cropping system, with spring corn (CC) and continuous winter wheat (LY and LF) growing in succession. Furthermore, the soil properties of the 0–20 cm soil layer at the first year of three long-term experiments are shown in Table S1. At each site, we selected conservation tillage practices (no tillage with straw return, NTS) and conventional tillage practices (plough tillage with straw removal, CT) for our study; the details of tillage management were as follows:

At the CC site, the experimental plot adopted a single factor split plot design with four replications. Each plot was 5.2 m wide and

20.0 m long. In the NTS practices, aside from the use of a no-till planter in late April to early May to ensure proper seed emergence, the field remained undisturbed throughout the year. To protect the soil from wind and water erosion, about 30–35 cm of maize stubble was retained after harvest in October, with uncut maize stalks evenly covering the soil surface and spaces between stubble under NTS. The CT practices involved moldboard ploughing to a depth of approximately 20 cm after maize harvest in autumn, followed by spring discing, cultivation, and ridge formation in June using a modified lister. All crop residues were removed from the field for use as fuel or animal feed and not returned to the soil under CT.

At the LY site, the experiment was conducted as a completely randomized design with three replications. Each plot measured 10 m in length and 3 m in width, with row spacing of 0.65 m. Under NTS, no tillage was performed year-round, leaving 30 cm of stubble after wheat harvest, and straw was evenly returned to the field as mulch after threshing. Under CT practices, wheat

**TABLE 1** | Study sites and soil properties of 0–20 cm soil depth at different locations.

Soil properties	Changchun (CC)	Luoyang (LY)	Linfen (LF)
Duration	2012–2021	1999–2021	1992–2017
Soil classification	Phaeozems	Calcaric Cambisols	Calcic Luvisols
Elevation (m)	195	324	450
Average annual temperature (°C)	4.4	13.7	13.3
Average annual rainfall (mm)	614	555	650
Particle size distribution (%)			
Sand (0.02–2 mm)	39.6	60.5	23.9
Silt (0.002–0.02 mm)	24.5	24.3	47.9
Clay (<0.002 mm)	35.9	15.2	28.2
Fertilization			
Nitrogen (kg ha <sup>-1</sup> )	150	45.5	78
Phosphorus (kg ha <sup>-1</sup> )	150	45.8	18
Potassium (kg ha <sup>-1</sup> )	225	65.5	—

was harvested with a stubble height of 5–6 cm, and both the straw and the grain were removed from the field. The field was ploughed annually to a depth of 20 cm in July without subsequent harrowing, followed by a second ploughing to the same depth before wheat sowing in September each year under CT, after which fertilization, harrowing and seeding were performed sequentially.

At the LF site, the experiment was conducted as a completely randomized design with three replications. Under both NTS and CT practices, 10–15 cm of wheat stubble was retained after harvest. In the NTS system, all wheat straw residues from the previous crop were left on the soil surface as mulch, and no soil disturbance occurred during the fallow period. In contrast, under CT, all wheat straw residues were removed, the soil was ploughed to a depth of 15–20 cm after harvest, and harrowing was conducted before sowing in October.

## 2.2 | Sampling

Soil samples were collected from the CC and LY sites at depths of 0–10 cm and 10–20 cm in October 2021, and from the LF site at the same depths in August 2017. All three sites have been maintained for over 10 years with consistent management (Table 1). A 2.64 cm diameter auger was used at five points in the “X” shape to collect soil samples, which were then mixed into a composite sample at each plot for the different treatments. To avoid potential heterogeneity, soil samples under NTS were taken from areas with uniform straw coverage and representative soil homogeneity. All soil samples are first screened to remove visible stones and straw residues and then divided into three parts. The first part of the samples was placed in an insulated box containing an ice pack and stored in a refrigerator at –20°C for the determination of microbial indicators. The second part of the soil sample was returned to the laboratory and air dried for the determination of physical and chemical indicators. The third part was

packed in a box to avoid compression and manually returned to the laboratory where it was dried to about 8%–10% moisture for aggregate screening (Dorodnikov et al. 2009; Kemper and Rosenau 1986). At harvest, wheat plants at the LY and LF sites were manually harvested from plots measuring 3 × 1 m<sup>2</sup>, and spring maize at the CC sites was harvested from plots measuring 1.2 × 5 m to determine crop yields, following the method described by Guan et al. (2015).

## 2.3 | Soil Physico-Chemical Properties

SOC and total nitrogen (TN) contents were determined using an elemental analyzer (Elementar, Germany) following the method of M. Zhang et al. (2022). Prior to analysis, all soil samples were ground, sieved through a 0.15 mm mesh, and treated with 1 M hydrochloric acid to remove inorganic carbon before determining SOC content. For the determination of soil available nitrogen (AVN, defined as the total content of NH<sub>4</sub><sup>+</sup>-N and NO<sub>3</sub><sup>-</sup>-N), 10 g of fresh soil was extracted with 2 M potassium chloride solution (soil-to-solution ratio of 1:5). The mixture was shaken on an oscillator at 200 rpm for 1 h (Hood-Nowotny et al. 2010). The filtrate was collected and analyzed using a continuous flow analyzer. Soil available phosphorus content (AVP, Olsen-P) was determined by extracting 2.5 g of soil with 0.5 M NaHCO<sub>3</sub> solution (soil-to-solution ratio of 1:20), shaking at 200 rpm for 30 min, and analyzing the extract according to the method described by Muukkonen et al. (2007).

Microbial biomass carbon (MBC) and microbial biomass nitrogen (MBN) were determined using the chloroform fumigation-extraction method (Nyamadzawo et al. 2009; Bailey et al. 2002). Fumigated and nonfumigated soil samples were extracted with 0.5 M K<sub>2</sub>SO<sub>4</sub>, and MBC and MBN were calculated by multiplying the difference in organic C by a kEC factor of 0.45. Soil pH was measured by equilibrating soil with ultrapure water and recording the value using a PB-10 electrode (Sartorius, Germany), following the procedure described by McLean (1982). To



calculate water content and bulk density, separate soil samples were taken from 0–10 cm and 10–20 cm soil layers using a core sampler (5 cm height, 4.5 cm diameter) and oven-dried at 105°C for 24 h (Lee et al. 2009).

## 2.4 | Soil Organic Carbon Storage and Carbon Sequestration Rate

SOC stocks ( $\text{Mg C ha}^{-1}$ ) were calculated using the equal mass method (Lee et al. 2009), and the soil weight of the CT treatment was used as the control. The  $\Delta$  SOC stock ( $\text{Mg C ha}^{-1}$ ) and SOC sequestration rate ( $\text{Mg C ha}^{-1} \text{ year}^{-1}$ ) at 0–20 cm soil depth were calculated as described by L. Gao et al. (2019) and Wendt and Hauser (2013) and expressed as follows:

$$H_{\text{add}} = \frac{BD_{\text{NTS}} - BD_{\text{CT}}}{BD_{\text{NTS}} * 10} \quad (1)$$

$$SOS_{\text{CT}} = SOC_{\text{CT}} * BD_{\text{CT}} * S * H * 10 \quad (2)$$

$$SOS_{\text{NTS}} = SOC_{\text{NTS}} * BD_{\text{NTS}} * S * (H + H_{\text{add}}) * 10 \quad (3)$$

where SOS, BD and SOC were the SOC stock ( $\text{Mg C ha}^{-1}$ ), soil bulk density ( $\text{g cm}^{-3}$ ), and carbon concentration ( $\text{g kg}^{-1}$ ) under different treatments,  $H$  (m) was the depth of the analyzed soil layer,  $H_{\text{add}}$  (m) was the depth of the soil layer to be corrected, and  $S$  is the soil area (ha).

$$\Delta \text{ SOC stock} = SOS_{\text{f}} - SOS_{\text{i}} \quad (4)$$

where the  $SOS_{\text{f}}$  and  $SOS_{\text{i}}$  indicated the SOC stocks in final and initial year under different tillage practices, respectively.

$$SOC_{\text{SR}} = \Delta \text{ SOC stock} / y \quad (5)$$

where the  $SOC_{\text{SR}}$  and  $y$  was the SOC sequestration rate and the duration of this field experiment.

## 2.5 | Aggregate Fraction

The soil samples passing through the 10-mm sieve were adjusted to a moisture content of approximately 8%–10% according to Kemper and Rosenau (1986). Subsequently, an amount equivalent to 50 g oven-dry soil was placed on the Automatic Sieve Shaker (Analysette 8411, Shaoxing, China) with 0.25 and 2-mm sieves and shaken for 2 min to collect the large macroaggregates (large macroaggregates:  $> 2$  mm), the small macroaggregates (small macroaggregates: 0.25–2 mm), and the microaggregates (microaggregates:  $< 0.25$  mm). It is believed that the dry sieving method avoids the hydraulic damage and leaching of dissolved organic matter from large aggregates in the wet sieving process (Sarker et al. 2018). The mean weight diameter (MWD) serves as a measure of aggregate stability and is calculated according to the following equation (L. Gao et al. 2019).

$$\text{MWD} = \frac{\sum_{i=1}^n (W_i \times X_i)}{\sum_{i=1}^n W_i} \quad (6)$$

where  $W_i$  (%) is the percentage by weight of soil aggregates in each size class, representing their proportion in the total sample, and  $X_i$  (mm) is the mean diameter of soil aggregates of different particle sizes.

## 2.6 | Carbon Functional Groups

The composition of the OC functional group in soil samples was measured using a Nicolet IS10 Fourier transform infrared (FTIR) spectrometer (Thermo Fisher). The bulk soil and the different particle size aggregates were oven-dried at 65°C for 5 h prior to being ground using a 100-mesh sieve. One milligram of the ground sample was then mixed with 100 mg of potassium bromide particles. Spectral recording was carried out using an average of 32 scans, with a wavelength resolution of  $4 \text{ cm}^{-1}$  and a range of 200–4000  $\text{cm}^{-1}$ . All spectra were baseline-corrected and normalized using OMNIC (v.8.0, Thermo Fisher Scientific) and visualized using Origin 2019. The semiquantitative approach used integrated peak areas (after uniform baseline correction and curve-fitting) to compute the relative proportion of each functional group (Soong et al. 2014; Szymański 2017). The percentage of a given band was calculated as:

$$\text{Relative Percentage of Peak A}(\%) = \frac{\text{Area}_A}{\sum_{i=A}^N \text{Area}_i} \times 100\% \quad (7)$$

where  $\text{Area}_A$  is the integrated area of the peak of interest (Margenot et al. 2023; Xue et al. 2019), and  $\sum_{i=A}^N \text{Area}_i$  is the sum of the integrated areas for all the functional group peaks being considered in the analysis.

## 2.7 | Iron Oxides, Exchangeable Calcium, and Specific Surface Area

The reactive iron (Fed) was extracted from bulk soil and different aggregate size fractions using the dithionite-citrate-bicarbonate (DCB) method, which selectively dissolves free and crystalline iron oxides (Inda et al. 2013). Treating soil samples with a sodium dithionite-citrate solution buffered by sodium bicarbonate under controlled conditions efficiently reduces and solubilizes iron oxides. The noncrystalline iron fraction (Feo) was extracted using the ammonium oxalate method at room temperature and in the dark to target amorphous and short-range ordered iron oxides without affecting crystalline forms (Barberis et al. 1991). Soil samples were extracted with  $1 \text{ mol L}^{-1}$  sodium acetate solution (NaOAc, pH 8.2) at a soil-to-solution ratio of 1:10 (w/v) to displace exchangeable calcium ions ( $\text{Ca}^{2+}$ ) (Houba et al. 2000). The concentrations of Fed, Feo, and  $\text{Ca}^{2+}$  under different treatments were determined by inductively coupled plasma atomic emission spectroscopy (ICP-AES; model 715-ES, Varian Inc., USA).

To determine the SSA of bulk soil and various aggregate size fractions, we employed multi-point Brunauer–Emmett–Teller (BET) analysis using an Autosorb surface area and porosimetry analyzer (Accelerated Surface Area and Porosimetry System, 2020, USA) with  $\text{N}_2$  gas as the adsorbate at 77 K. Prior to analysis, samples were degassed under vacuum with helium at 40°C

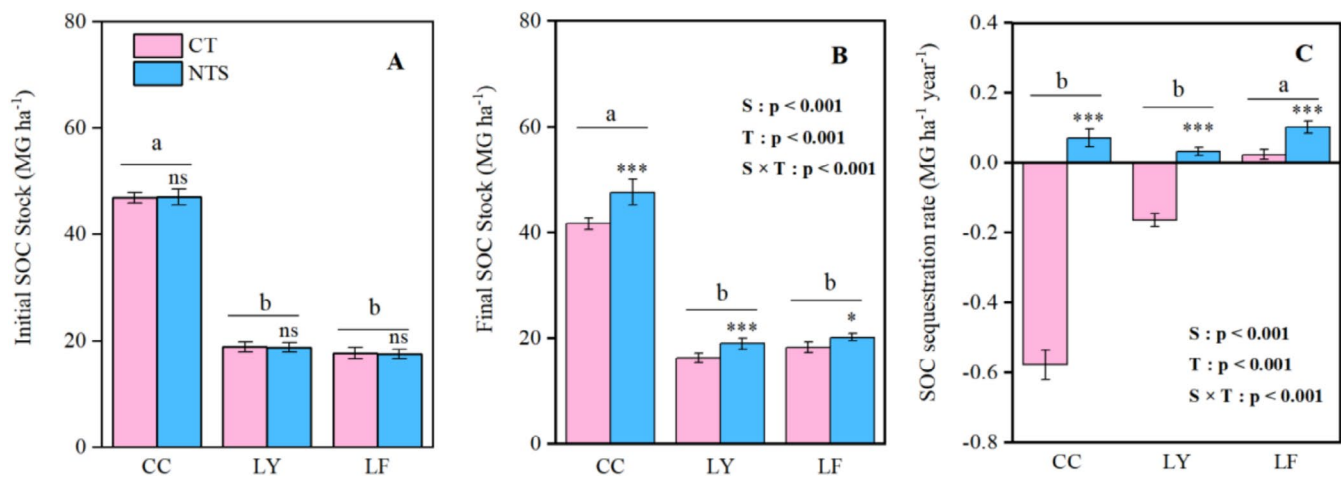


**FIGURE 2** | The initial and final soil organic carbon stock and sequestration rate at 0–20 cm soil depth under conventional tillage with straw removal (CT) and no tillage with straw return (NTS) at three different sites. CC: Changchun (Phaeozems, 2012–2021), LY: Luoyang (Calcic Cambisols, 1999–2021), and LF: Linfen (Calcic Luvisols, 1992–2017). Different lowercase letters indicate significant differences between three sites ( $p < 0.05$ ). Asterisks indicate significant differences between NTS and CT. S: Study site; T: Tillage; the  $S \times T$  represent the interaction effects ( $*p < 0.05$ ,  $**p < 0.01$ ,  $***p < 0.001$ ).

for 12 h. To remove organic carbon from the size fractions, each was treated four times for 6 h with 1 M NaOCl (pH 8) at a soil-to-solution ratio of 1:50. The treated samples were then washed with deionized water until the electrical conductivity was below  $50 \mu\text{S cm}^{-1}$ , freeze-dried, and subsequently analyzed for SSA following the method of Schweizer et al. (2019).

## 2.8 | Statistical Analysis

Statistical analyses were performed using the SPSS 30.0 software package (IBM, USA). A general linear model (GLM) was used to conduct analysis of variance (ANOVA), using multivariate analysis followed by Tukey's honest significant difference (HSD) test at  $p < 0.05$ , to evaluate significant differences and interactions among various indicators across different tillage practices, soil types, and soil depths. Data were tested for normality and homogeneity of variances using the Shapiro–Wilk and Levene's tests, respectively, before conducting ANOVA. Pearson correlation analysis was used to examine the relationships between soil minerals and organic carbon functional groups. Random Forest regression models were employed to estimate the main biochemical predictors of changes in crop yield using the “rfPermute” package (R version 4.4.0). This method effectively captures complex relationships, reduces overfitting, and identifies important variables influencing final SOC storage (Speiser et al. 2019). Partial least squares path modeling (PLS-PM) was performed to reflect the complex regulatory effects of main factors on aggregate stability and SOC sequestration using the “plsmpm” package (R version 4.4.0). Data visualization was conducted using Origin 22.0 software.

## 3 | Results

### 3.1 | Soil Carbon Storage and Sequestration Rate

We compared the initial and final years of SOC stock at different sites (Figure 2). Among the three sites, CC exhibited the largest initial SOC stock in the 0–20 cm soil layer. Compared to CT, NTS

significantly increased the final SOC stock by 28.4%, 15.8%, and 10.2% at the LY, CC, and LF sites, respectively. Additionally, NTS enhanced the SOC sequestration rate by 15.3%–76.7% across the three sites. In contrast, under CT, SOC stock declined at the CC (14.2%) and LY (23.8%) sites compared to the initial year. The positive sequestration rates under NTS highlight its long-term beneficial impact on SOC stock. The interaction between tillage practices and sites revealed that the SOC stock increase due to NTS was greater at LY (17.6%) than at CC (14.3%) and LF (11.1%), suggesting that Calcic Cambisols respond more positively to conservation tillage. Moreover, the highest SOC sequestration rate observed at the LF site reflects a greater potential for carbon sequestration in Calcic Luvisols under long-term NTS than the initial year.

### 3.2 | Soil Physical and Chemical Properties in Different Sites

Generally, the topsoil (0–10 cm) had larger contents of SOC, MBC, TN, and MBN, but lower bulk density and pH compared to the subsoil (10–20 cm). NTS resulted in a slightly lower soil pH than CT at the CC and LF sites, and in the topsoil layer at LY (Table 2). At all three sites, NTS significantly increased the contents of SOC, TN, MBC, and AVN in the topsoil compared to CT. In the subsoil, NTS also led to a 12.7% increase in SOC content at the LY site and significantly enhanced AVP by 55.4% at CC and 28.4% at LY. Moreover, NTS increased MBC and MBN contents by 14.3%–41.2% in both the 0–10 cm and 10–20 cm layers at the CC and LF sites relative to CT.

Among the three sites, soil pH was lowest at the CC site compared to LY and LF. Moreover, the contents of SOC, MBC, MBN, TN, and AVN were largest at CC, while LY and LF exhibited similar levels of these indicators. According to the interaction effects, the impact of NTS on BD, SOC, MBC, MBN, and AVP was more pronounced in the topsoil than in the subsoil. However, the effects of NTS on these indicators varied among regions. Notably, NTS reduced bulk density in the subsoil only

TABLE 2 | Soil physical and chemical properties in the 0–20 cm depth of different sites and tillage practices.

Sites	Soil depths (cm)	Tillage	pH	BD (g cm <sup>-3</sup> )	SOC (g kg <sup>-1</sup> )	MBC (mg kg <sup>-1</sup> )	TN (g kg <sup>-1</sup> )	MBN (mg kg <sup>-1</sup> )	AVN (mg kg <sup>-1</sup> )	AVP (mg kg <sup>-1</sup> )
CC	0–10 cm	CT	6.93a	1.27ab	16.50b	305.05b	1.38b	38.51b	38.21b	29.26d
		NTS	6.84a	1.33ab	21.43a	420.76a	1.65a	52.73a	48.93a	65.61a
	10–20 cm	CT	7.01a	1.37a	14.72b	284.85c	1.29c	32.45c	32.85c	37.19b
LY	0–10 cm	NTS	6.85a	1.24b	15.41b	332.71b	1.38c	37.96b	43.96b	30.85c
		CT	8.42a	1.13ab	7.21b	165.2b	0.75b	33.23a	14.89b	27.48b
	10–20 cm	NTS	8.11b	1.06b	9.47a	216.8a	0.96a	32.83a	20.16a	38.39a
LF	0–10 cm	CT	8.34ab	1.21a	6.68c	131.6c	0.72b	31.83b	14.42b	26.23b
		NTS	8.52a	1.17ab	7.61b	116.4c	0.68b	31.86b	23.66a	35.25a
	10–20 cm	CT	7.97a	1.36b	6.53b	165.12b	0.69b	30.01b	14.17c	41.2a
	0–10 cm	NTS	7.65b	1.42ab	8.02a	222.62a	0.81a	44.72a	22.01a	30.70c
		CT	8.01a	1.51a	6.21b	81.71c	0.59c	15.62d	16.02b	19.35d
	10–20 cm	NTS	7.78ab	1.44ab	6.07b	139.13b	0.64bc	20.09c	15.94b	37.91b
Source of variability		df	F							
S		2	318.5***	378.5***	2325.6***	811.5***	1042.0***	73.8***	622.3***	55.7***
D		1	11.0**	14.4***	154.5***	160.0***	55.2***	51.2***	137.0***	151.4***
T		1	2.3	56.6***	235.3***	260.4***	124.2***	158.0***	11.8**	99.3***
S×D		2	1.8	3.0	20.5***	18.2***	5.7**	14.7***	10.2***	16.4***
S×T		2	0.6	10.4***	45.1***	3.8*	0.8	35.1***	10.6***	19.3***
D×T		1	3.3	32.7***	78.1***	28.3***	29.3***	12.3**	1.1	10.9**
S×D×T		2	3.0	15.5***	11.0***	7.6**	5.0*	4.1*	8.1**	178.9***

Note: Different lowercase letters indicate site-specific significant differences between tillage practices and two soil depths at each site ( $p < 0.05$ ). All  $F$ -values, sources of variability, degrees of freedom (df) and significance levels are derived from the statistical analysis output. Asterisks denote the level of significance: \* $p < 0.05$ , \*\* $p < 0.01$ , \*\*\* $p < 0.001$ ;  $D$ : soil depth;  $T$ : tillage;  $S \times D$ ,  $S \times T$ ,  $D \times T$  and  $S \times D \times T$  represent the interaction effects. Abbreviations: AVN, available nitrogen; AVP, available phosphorus; BD, bulk density; CC, Changchun (Phaeozems); CT, conventional tillage (plough tillage with straw removal); LF, Linfen (Calcic Luvisols); LY, Luoyang (Calcic Cambisols); MBC, microbial biomass carbon; MBN, microbial biomass nitrogen; NTS, no tillage with straw return; SOC, soil organic carbon; TN, total nitrogen.

at the CC site. More importantly, the increase in total SOC due to NTS was greatest at the LY site, whereas the enhancements in MBC and MBN were most pronounced at the LF site.

### 3.3 | Aggregate-Associated Carbon and Nitrogen Content

In general, long-term NTS promoted the formation of macroaggregates and improved aggregate stability in the 0–10 cm and 10–20 cm soil layers. NTS increased the proportion of large macroaggregates by 12.2%–14.9% in the two soil layers at CC and LY sites. Moreover, the proportion of small macroaggregates increased by 7.6%–15.3% and that of microaggregates reduced by 18.6%–25.2% under NTS compared to CT at LY and LF sites. This change under NTS resulted in significantly larger MWD in both soil layers than CT (Figure S1d). At different sites, CC had the greatest proportion of large macroaggregates and the smallest proportion of microaggregates, thus significantly increasing MWD values compared to LY and LF in both soil layers (Figure S1d).

At all sites, NTS significantly increased SOC and TN storage in macroaggregates compared to CT across both soil layers (Figure 3D–I). Specifically, NTS increased SOC and TN in total large and small macroaggregates by 17.8%–28.3% at the CC site and by 21.2%–46.3% at the LY site. At the LF site, NTS enhanced SOC and TN by 17.1%–33.5% in small macroaggregates compared to CT. In different sites, CC had the greatest SOC and TN contents in large macroaggregates and the least in microaggregates, compared to LY and LF across both soil layers (Figure 3D–I). The interaction effects between tillage and site revealed that NTS led to the greatest increases in MWD (12.7%) and macroaggregate-associated SOC (37.0%) and TN (22.6%) at the LY site, compared to CC (6.4%, 22.6%, 18.8%) and LF (7.6%, 31.4%, 11.1%). Moreover, NTS significantly increased SOC content in microaggregates at the CC site, whereas both the SOC and TN contents were significantly reduced in microaggregates under the LF site at 0–10 cm and under the LY site at 10–20 cm soil layer.

### 3.4 | Carbon Functional Groups and Minerals

We determined the SOC functional groups in bulk soil, macroaggregates and microaggregates (Table 3). The main SOC functional groups were classified into phenolic-C, aliphatic-C, aromatic-C, carboxy-C, and polysaccharide-C in different fractions. In the bulk soil, NTS significantly increased the aromatic-C/aliphatic-C ratio by 8.9%–42.2% at three sites compared to CT. Furthermore, NTS had a significantly larger aliphatic-C, polysaccharide-C percentage and smaller phenol-C percentage than CT at CC and LY sites. The interaction effect between aggregate and tillage showed that, in the macroaggregates, NTS increased the aromatic-C percentage and the aromatic-C/aliphatic-C ratio by 5.9%–41.8% at all the sites. In contrast, in microaggregates, NTS significantly decreased the aromatic-C/aliphatic-C ratio.

Among the three sites, CC showed a larger average aliphatic-C, aromatic-C, and polysaccharides-C and a smaller phenolic-C percentage than the LY and LF sites. The interaction effects between site (S) and tillage (T) were highly significant

( $p < 0.001$ ) for carboxyl-C, aliphatic-C, and aromatic-C. For carboxyl-C, NTS reduced its content in both bulk soil and macroaggregates at the CC and LY sites but increased it in macroaggregates at the LF site. NTS consistently promoted aromatic-C in both bulk soil and macroaggregates at the CC and LY sites, whereas its effect was not significant at the LF site. In contrast, at the LF site, NTS reduced the proportions of both aliphatic-C and aromatic-C in large macroaggregates. This led to a consistent increase in the relative aromatic-C/aliphatic-C under NTS across different sites. A key feature of the three-way interaction is that the effect of NTS on the aromatic-C/aliphatic-C ratio in bulk soil was most pronounced at the LY site, while its reduction effect in microaggregates was stronger at the CC and LY sites than at the LF.

### 3.5 | Iron Oxides, Exchangeable Ca and Specific Surface Area

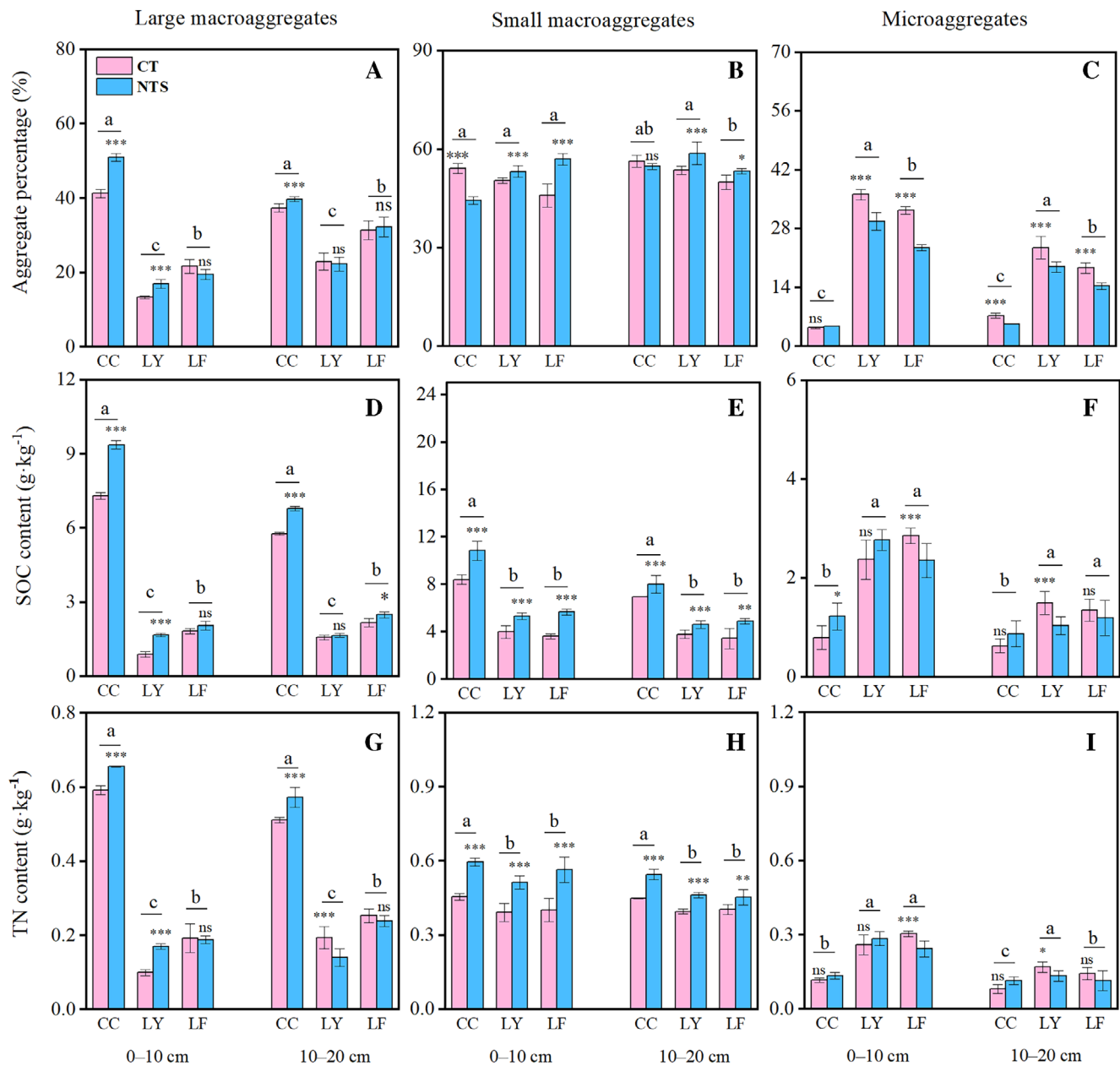
The 0–10 cm soil layer exhibited greater levels of Fed, Feo, exchangeable  $\text{Ca}^{2+}$ , and SSA than the 10–20 cm layer across all sites and tillage treatments. Among the sites, NTS significantly reduced Fed content, while increasing Feo, exchangeable  $\text{Ca}^{2+}$  and SSA in bulk soils compared to CT (Figure 4). The effects of NTS on soil iron minerals varied among regions. Specifically, Feo content increased by 31.5% at CC, 23.5% at LY, and 15.1% at LF under NTS relative to CT. Exchangeable  $\text{Ca}^{2+}$  content also increased by 18.6%–27.4% under NTS at the LY and LF sites but showed no significant difference at the CC site. Similar to SOC and TN, the CC site consistently exhibited the greatest levels of Fed, Feo, exchangeable  $\text{Ca}^{2+}$ , and SSA compared to LY and LF. Additionally, the LY site had smaller SSA in macroaggregates than the LF site. No significant differences in SSA between NTS and CT were observed in the microaggregates at the LF site.

We used the Pearson correlation method to analyze the relationships between different minerals and organic carbon functional groups (Figure 5). The results showed that polysaccharide-C was positively correlated with Feo, exchangeable  $\text{Ca}^{2+}$  content, and SSA, but negatively correlated with Fed content. Aliphatic-C showed positive correlations with both Fed and exchangeable  $\text{Ca}^{2+}$  content. Aromatic-C and the aromatic-C/aliphatic-C ratio were significantly negatively correlated with Fed, but positively correlated with Feo, exchangeable  $\text{Ca}^{2+}$  content, and SSA. In contrast, carboxyl-C was negatively correlated with Feo, exchangeable  $\text{Ca}^{2+}$  content, and SSA, but positively correlated with Fed content.

### 3.6 | Relationship Between Soil Physico-Chemical Properties and Carbon Storage

We employed Random Forest analysis to identify key predictors of SOC storage (Figure 6A). The model explained 90.5% of the variation in SOC storage. Among the predictors, Feo, Fed, carboxyl-C proportion, and exchangeable  $\text{Ca}^{2+}$  content were the most significant contributors to SOC storage ( $p < 0.01$ ). In addition, aromatic-C, MWD, the aromatic-C/aliphatic-C ratio, and polysaccharide-C also significantly influenced SOC storage ( $p < 0.05$ ; Figure 6A). Moreover, the SOC content showed





Terms	Source of Variability						
	S	A	T	S × A	S × T	A × T	S × A × T
A ggregate percentage	951.0***	--	0	54.7***	67.3***	--	--
SOC content	1184.3***	623.1***	126.3***	149.6***	172.2***	16.9***	47.6***
TN content	208.0***	47.9***	5.1*	3.6*	19.0***	0.2	2.2

**FIGURE 3** | The percentage of different aggregate particle size classes (A–C), the storage of soil organic carbon (SOC, D–F) and total nitrogen (TN, G–I) within different aggregate size classes at 0–20cm soil depth under conventional tillage (plough tillage with straw removal, CT) and no tillage with straw return (NTS) at three different sites. CC: Changchun (Phaeozems), LY: Luoyang (Calcaric Cambisols), and LF: Linfen (Calcic Luvisols). Different lowercase letters indicate significant differences between three sites ( $p < 0.05$ ). Asterisks indicate significant differences between NTS and CT. All  $F$ -values, sources of variability, degrees of freedom (df) and significance levels are derived from the statistical analysis output.  $S$ : Study site;  $A$ : Aggregate fractions;  $T$ : Tillage;  $S \times A$ ,  $S \times T$ ,  $A \times T$  and  $S \times A \times T$  represent the interaction effects (\* $p < 0.05$ , \*\* $p < 0.01$ , \*\*\* $p < 0.001$ ).

a positive relationship to MWD, TN content, aromatic-C, polysaccharide-C and the ratio of aromatic-C/aliphatic-C, and a negative relationship to phenolic-C percentage (Figure S2). These results indicate that SOC sequestration is positively influenced by aggregate stability and associated carbon functional groups.

Finally, we used the PLS-PM method to analyze the direct and indirect effects of different effective predictors on SOC storage under conservation tillage practices (Figure 6B). We found that NTS contributed positively to the levels of available nutrients (AVN + AVP) and microbial biomass (MBC + MBN), Feo and

TABLE 3 | Fourier-transform infrared spectra for the different fractions in the 0–20 cm depth of different sites and tillage practices.

Sites	Fractions	Tillage	Phenolics-C		Aliphatic-C		Aromatic-C		Carboxyl-C		Polysaccharide-C		Aromatic-C/ Aliphatic-C
			3416 cm <sup>-1</sup>	2930–2853 cm <sup>-1</sup>	1637 cm <sup>-1</sup>	1444 cm <sup>-1</sup>	1085, 1032 cm <sup>-1</sup>						
CC	Bulk soil	CT	39.65a	0.70ab	5.47bc	4.58a	49.63b	7.81c					
		NTS	36.32b	0.77a	6.07ab	3.27b	53.58a	7.93bc					
	Macroaggregates	CT	42.13a	0.68b	5.31c	3.52b	48.43b	7.75c					
		NTS	36.34b	0.77a	6.75a	3.78b	52.38a	8.77b					
LY	Microaggregates	CT	36.85b	0.58c	5.78b	2.98c	54.22a	9.96a					
		NTS	39.72a	0.76a	5.93b	4.14ab	49.59b	7.80c					
	Bulk soil	CT	44.09c	0.49a	2.77c	11.70a	40.96c	5.66c					
		NTS	47.26b	0.39b	3.20ab	8.44cd	40.71c	8.28b					
LF	Macroaggregates	CT	50.92a	0.48a	3.11b	9.19c	36.30d	6.54c					
		NTS	48.67ab	0.51a	3.52a	7.89d	39.41c	6.95bc					
	Microaggregates	CT	43.54c	0.30c	2.94bc	10.07b	43.15b	9.73a					
		NTS	41.29d	0.37b	2.65c	9.08c	46.62a	7.15c					
	Bulk soil	CT	39.74c	0.42c	2.48c	11.51a	45.84ab	5.88b					
		NTS	40.99bc	0.40cd	2.59c	11.11a	44.92b	6.46a					
	Macroaggregates	CT	45.05a	0.71a	3.11a	8.87b	42.25c	4.38c					
		NTS	42.20b	0.43c	2.74b	11.39a	43.24c	6.42a					
	Microaggregates	CT	39.12c	0.38d	2.56c	10.68a	47.26a	6.78a					
		NTS	42.71b	0.52b	2.88ab	11.18a	42.72c	5.57b					
Source of variability		df	F										
S		2	35.8***	73.1***	1007.2***	459.5***	59.6***	13.5***					
A		2	9.6**	9.9***	11.0***	8.2***	7.3***	28.9***					
T		1	2.58	7.53*	23.8***	2.5	0.5	3.5*					
S×A		4	3.14	14.5***	1.4	3.3*	2.0	12.7***					
S×T		2	0.75	10.2***	18.5***	38.9***	1.5	3.0					
A×T		2	5.7**	17.6***	5.4**	12.8***	3.5*	83.4***					
S×A×T		4	2.1	14.9***	11.0***	4.3**	2.3	20.5***					

Note: Different lowercase letters indicate site-specific significant differences between tillage practices and aggregate fractions at each site ( $p < 0.05$ ). All  $F$ -values, sources of variability, degrees of freedom (df) and significance levels are derived from the statistical analysis output. Asterisks denote the level of significance: \* $p < 0.05$ , \*\* $p < 0.01$ , \*\*\* $p < 0.001$ . S: study site; A: aggregate fractions; T: tillage; S×A, S×T, A×T and S×A×T represent the interaction effects. Abbreviations: CC, Changchun (Phaeozems); CT, conventional tillage (plough tillage with straw removal); LF, Lintfen (Calcic Luvisols); LY, Luoyang (Calcic Cambisols); NTS, no tillage with straw return.

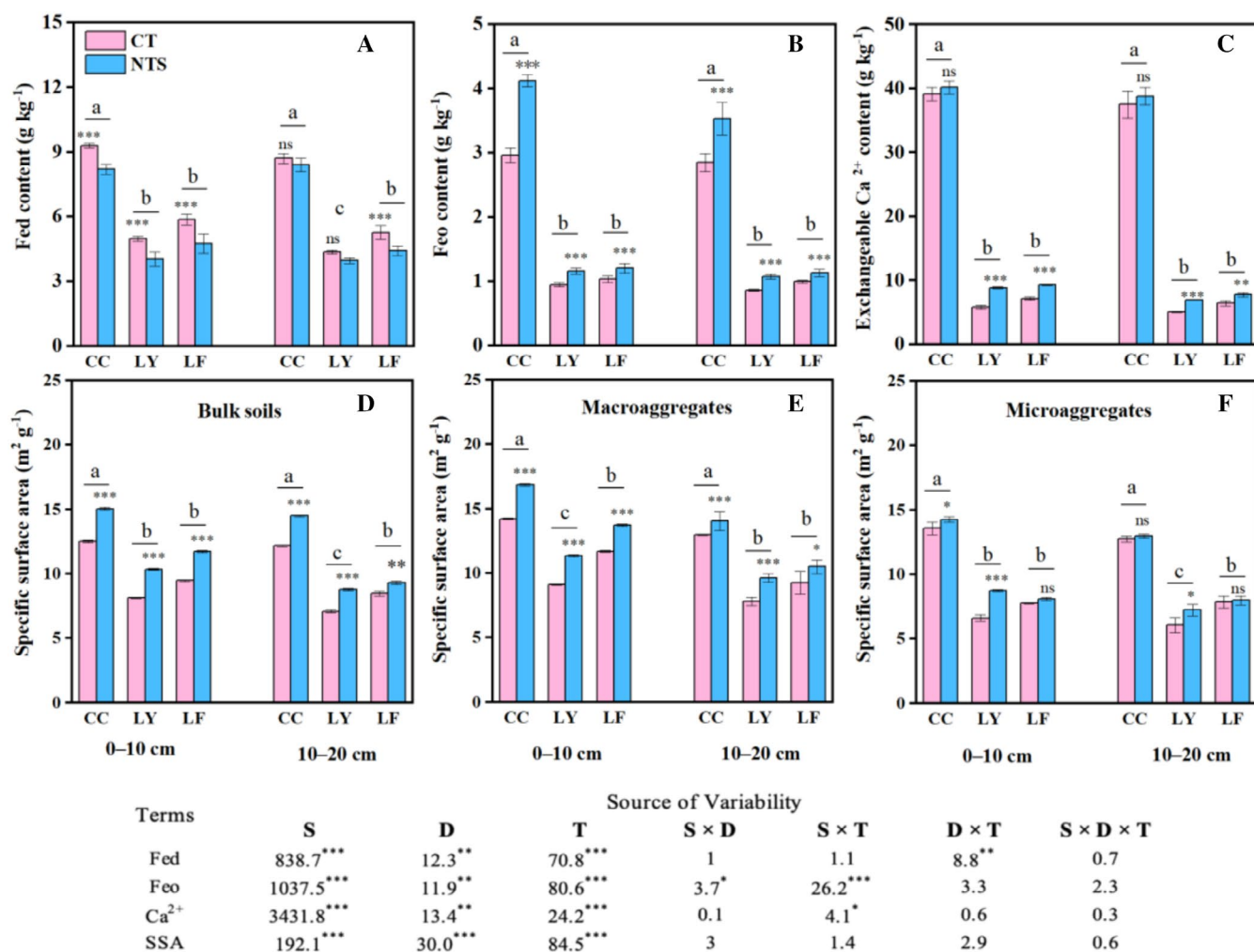


**FIGURE 4** | The free iron content (Fed, A), amorphous iron content (Feo, B), exchangeable calcium content (Ca<sup>2+</sup>, C) and specific surface area (SSA) of bulk soils and aggregates (D–F) under conventional tillage (plough tillage with straw removal, CT) and no tillage with straw return (NTS) at three different sites. CC: Changchun (Phaeozems), LY: Luoyang (Calcic Cambisols), and LF: Linfen (Calcic Luvisols). Different lowercase letters indicate significant differences between three sites ( $p < 0.05$ ). Asterisks indicate significant differences between NTS and CT. All  $F$ -values, sources of variability, degrees of freedom (df) and significance levels are derived from the statistical analysis output.  $S$ : Study site;  $D$ : Soil depth;  $T$ : Tillage;  $S \times D$ ,  $S \times T$ ,  $D \times T$  and  $S \times D \times T$  represent the interaction effects (\* $p < 0.05$ , \*\* $p < 0.01$ , \*\*\* $p < 0.001$ ).

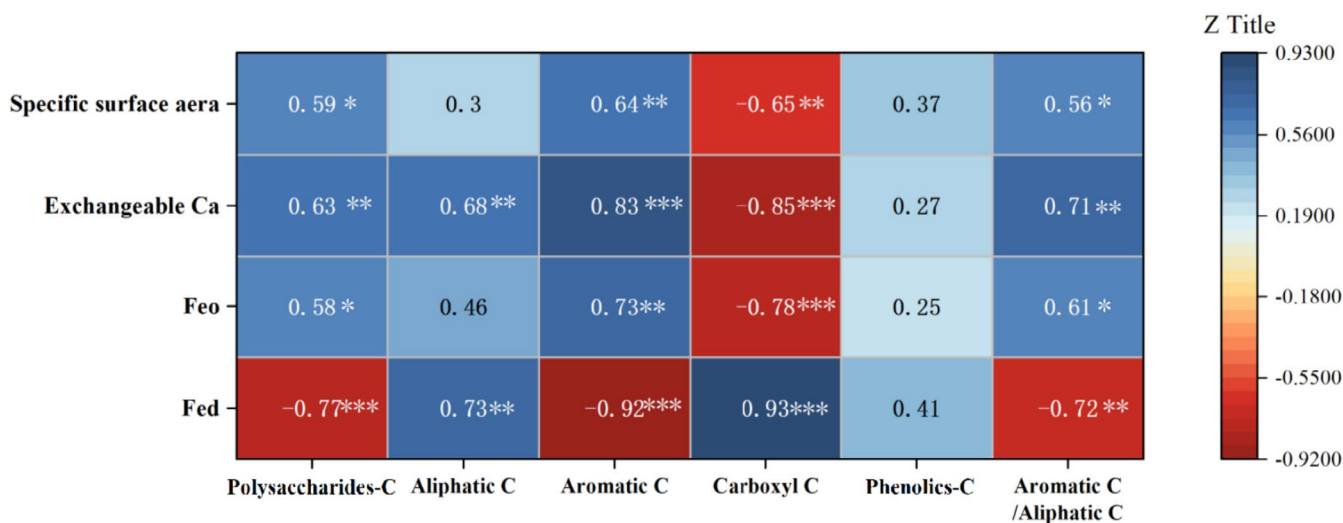


**FIGURE 5** | Pearson correlation analysis was conducted on mineral ion composition and organic carbon chemical functional groups under different tillage practices and sites. Asterisks indicate correlation coefficients between different indicators (\* $p < 0.05$ , \*\* $p < 0.01$ , \*\*\* $p < 0.001$ ).

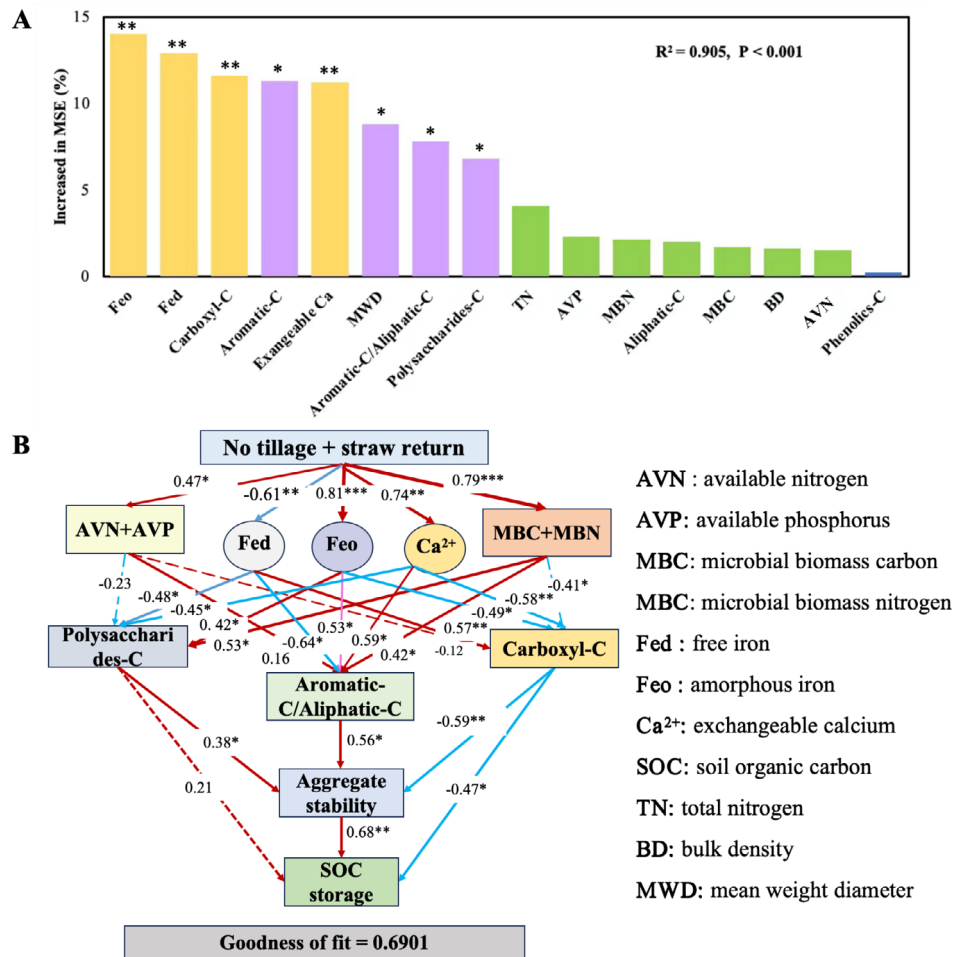


**FIGURE 6** | Identification of key predictors for soil organic carbon storage using Random Forest analysis (A). Partial least squares path modeling (PLS-PM) analysis of the relationships between soil physicochemical properties and soil organic carbon storage under different sites and tillage practices (B). Pink lines indicate positive effects, and blue lines represent negative effects. The values on the arrows indicate the strength of the relationships between variables (path coefficients). Asterisks indicate statistically significant relationships (\* $p < 0.05$ , \*\* $p < 0.01$ , \*\*\* $p < 0.001$ ).

exchangeable Ca contents, and negatively to Fed contents in this study ( $p < 0.05$ ). Furthermore, Feo, exchangeable Ca, microbial biomass, and available nutrients contributed to a higher ratio of aromatic-C/aliphatic-C under NTS. The Fed showed a positive relationship with carboxy-C content. However, Feo, exchangeable Ca, MBC + MBN positively correlated with polysaccharide-C and negatively correlated with carboxy-C percentage. The carboxy-C negatively contributed to aggregated stability and SOC content ( $p < 0.05$ ). Overall, the higher polysaccharide-C and aromatic-C/aliphatic-C ratio promoted aggregate formation, thus contributing significantly to the final SOC storage.

## 4 | Discussion

### 4.1 | The Effects of Conservation Tillage Practices on SOC Sequestration

Conservation tillage minimizes anthropogenic soil disturbance and promotes surface residue retention, thereby preserving soil structural integrity and enhancing pedospheric stability (Wang et al. 2020). It also improves soil physical properties and reduces losses of nutrients and soil moisture, thus promoting

soil quality and long-term functionality (Engell et al. 2022). In this study, long-term NTS increased SOC content and storage in the topsoil across different soil types compared to conventional tillage. Furthermore, NTS enhanced the annual mean SOC sequestration rate relative to the initial year (Figure 2C). The input of straw plays a crucial role, as it introduces organic matter directly to stimulate microbial growth, enhance soil nutrient availability and increase the mineral ion content, thereby stimulating carbon and nitrogen cycling (Hao et al. 2022). In our study, MBC and MBN were significantly larger under NTS (Table 2), which facilitated microbial decomposition and transformation of straw, subsequently leading to increased SOC storage. More importantly, the preservation of NTS on SOC was mainly attributed to the combined effects of physical protection by soil aggregates and the formation of stable carbon chemical composition. We found that NTS increased the proportion of macroaggregates and the associated SOC storage within the bulk soil (Figure 3). It has been reported that large macroaggregates contribute the majority of the carbon pool in conservation systems (Kan et al. 2020). Consistently, no-tillage practices have been shown to enhance large aggregate stability and total carbon sequestration in black soil (S. Zhang et al. 2012) and in paddy soil (Xue et al. 2019). Moreover, NTS



enhanced the content of Feo at three sites and the SSA of soil aggregates (Figure 4). Typically, these soil minerals, through adsorption and co-precipitation, bind with small organic molecules and form stable organo-mineral complexes that resist microbial degradation and persist (Adhikari and Yang 2015; Hartmann and Six 2023). The greater SSA under NTS further contributed to carbon sequestration and SOC stabilization. Taken together, our study highlights that conservation tillage enhances SOC storage by promoting aggregate-mediated protection, nutrient enrichment, and chemical stabilization, making it an effective strategy to mitigate SOC loss and sustain productivity across soil types.

In different sites, the CC (Phaeozems) showed a higher large macroaggregate proportion and total SOC storage than LY (Calcaric Cambisols) and LF (Calcic Luvisols) under NTS (Figure 2). The stabilization potential of SOC is influenced by soil texture and mineral composition. Typically, clay soils, compared with sandy loam, are more prone to particle aggregation, facilitating macroaggregate formation and stabilizing soil structure (Schweizer et al. 2019). In our study, Phaeozems exhibited greater clay content, with macroaggregate percentages ranging from 42.4% to 56.3%, significantly enhancing aggregate stability and SOC protection (Figure 3). Additionally, recent studies highlight the increasing importance of soil mineral ions in long-term SOC stabilization (Xiao et al. 2023). Certain ions, such as Fe oxides,  $\text{Ca}^{2+}$  and  $\text{Mg}^{2+}$ , not only act as inorganic binding agents, promoting macroaggregate formation, but also selectively adsorb SOC via adsorption and co-precipitation mechanisms, forming persistent, mineral-associated organic matter (Shabtai et al. 2023). Phaeozems had the largest concentrations of free iron, amorphous iron, and exchangeable calcium, along with a significantly increased SSA (Figure 4). This enhanced the adsorption capacity for straw-derived small molecules and microbial residues, thereby improving carbon stabilization potential. Phaeozems exhibited superior carbon sequestration potential compared with other regions due to physical and chemical protection in this study.

#### 4.2 | Soil Minerals Influenced Carbon Chemical Composition Under Different Tillage and Soil Types

At the three sites, NTS increased the ratio of aromatic-C/aliphatic-C in bulk soil (Table 3). A larger aromatic-C/aliphatic-C ratio is generally interpreted as indicating more chemically complex and stable organic matter, contributing to longer-term carbon persistence in soils (Spaccini et al. 2000). We found that NTS enhanced the aromatic-C proportion in bulk soil and macroaggregates in the CC and LY sites (Table 3). This may be attributed to the additional input of straw and its varying degrees of microbial decomposition. Aromatic-C typically originates from chemically stable organic compounds such as lignin and humic substances, with lignin being a major structural component of straw residues (Sowers et al. 2018). In addition, SOC functional groups originate from plant residues and decomposition products, which are further transformed by soil fungi and bacteria into more stable forms such as aromatic-C (Almagro et al. 2021). The greater crop productivity commonly observed under NTS increases root biomass and exudate input (Figure S4), which in turn stimulates microbial metabolism and is more likely to

promote the formation of chemically stabilized carbon compounds (Cotrufo et al. 2013; C. Liang et al. 2019). Therefore, NTS facilitates the retention of surface residues, reduces disturbance and increases crop yield, which support the accumulation of recalcitrant organic compounds.

In Calcaric Cambisols and Phaeozems, CT reduced the content of polysaccharide-C in both bulk soil and macroaggregates (Table 3). Polysaccharide-C, mainly derived from cellulose and hemicellulose, is highly biodegradable and sensitive to external disturbances such as tillage and moisture fluctuation (Kögel-Knabner 2017; Cotrufo et al. 2015). Our study indicates that NTS increased MBC and MBN (Table 2), suggesting enhanced microbial activity. This microbial stimulation may have facilitated the decomposition of straw into both labile and stable organic molecules. Thus, the accumulation of polysaccharide-C under NTS may be attributed to increased microbial secretion of extracellular polysaccharides stimulated by retained straw residues, along with reduced soil disturbance and greater aggregate physical protection. Conversely, NTS resulted in smaller carboxyl-C content in both Phaeozems and Calcaric Cambisols (Table 3). Under CT, the removal of surface residues often leads to greater reliance on root exudates, which are typically rich in carboxyl-containing compounds (Kögel-Knabner 2017; Cotrufo et al. 2015). Carboxyl-C is sensitive to soil pH because of the ionization of carboxyl groups (Witzgall et al. 2021; Dou et al. 2023). We observed slightly lower pH values under NTS compared to CT (Table 2). Consistently, Kan et al. (2022) and Zhou et al. (2022) reported that long-term no tillage may reduce pH, facilitating polysaccharide-C transformation into carboxyl-C under alkaline conditions.

Minerals can selectively adsorb OC functional groups depending on ion valence states and mineral-SSA (Cai et al. 2022). In our results, aromatic-C and the aromatic-C/aliphatic-C ratio showed a negative correlation with Fed but a positive correlation with Feo and  $\text{Ca}^{2+}$  (Figure 5). Hydroxyl (-OH) or phenolic hydroxyl (-OH) groups in aromatic-C can bind with Fe oxides (such as goethite and hematite) through hydrogen bonding or surface complexation, enhancing SOC stability (Zhou et al. 2022). In this study, NTS enhanced Feo content as well as the aromatic-C/aliphatic-C ratio. The strong positive correlation between Feo and aromatic-C content suggests that Feo may selectively bind to aromatic-C structures for greater SOC chemical stability under NTS. In different sites, the Phaeozems had the largest Feo and exchangeable Ca content, accompanied by an increase in aromatic-C and the aromatic-C/aliphatic-C ratio (Figure 4; Table 3). This is partly because the Phaeozems in northern China developed from wetlands, where shifts between anaerobic and aerobic conditions enhanced  $\text{Fe}^{2+}$  oxidation (S. Zhang et al. 2012). Meanwhile, low temperatures at the CC site reduced microbial activity, slowing straw decomposition and leading to lignin accumulation (Zhou et al. 2022). However, as noted above, increased exchangeable  $\text{Ca}^{2+}$  under NTS was observed only at the LF and LY sites (Figure 4). In the calcium-rich soils,  $\text{Ca}^{2+}$  can form calcium bridges with carboxyl and phenolic hydroxyl groups, thereby stabilizing organo-Ca associations (Wan et al. 2021). Phenolic-C and carboxyl-C were greater in Calcaric Cambisols and Calcic Luvisols but less in Phaeozems (Table 3). Taken together, these findings suggest that Feo oxides and exchangeable Ca contribute to increased soil SSA and selectively

interact with organic carbon functional groups, thereby enhancing SOC chemical stabilization.

### 4.3 | Minerals and Organic Carbon Functional Groups Regulate Aggregate Stability to Enhance SOC Storage

We found that NTS promoted macroaggregate formation and enhanced aggregate stability across different sites (Figure 3). PLS-PM analysis further revealed that Feo, exchangeable Ca, and MBC were positively associated with aggregate stability (Figure 6B). The stability of aggregates is closely linked to bonding materials, including inorganic binders and organic compounds (Xue et al. 2019). Continuous crop residue input provides a rich substrate for microbial activity, enhancing bioproduct release through residue decomposition and root exudation (Y. Gao et al. 2023). This, in turn, promotes clay and silt aggregation, stimulates fungal hyphae formation, and increased soil macroaggregate content under NTS. In addition, NTS increased FeO and exchangeable Ca levels, which contributed to increased SSA in both bulk soil and macroaggregates (Figure 4). Under NTS, greater humus levels can complex with  $\text{Fe}^{3+}$ , inhibiting the crystallization of Feo into Fed (Inda et al. 2013). Moreover, increased soil moisture under NTS may create micro-reducing conditions that promote  $\text{Fe}^{3+}$  reduction to  $\text{Fe}^{2+}$ , which can then re-oxidize and form Feo through microbial oxidation (Li et al. 2022). The studied Cambisols and Calcic Luvisols had a high pH and contained a large proportion of calcium carbonate. When soil moisture increases and pH relatively decreases, calcium carbonate tends to dissolve and release  $\text{Ca}^{2+}$  (Ball et al. 2023). In our study, NTS reduced soil pH in the topsoil at the LY and LF sites (Table 1), which may have induced this transformation and the associated  $\text{Ca}^{2+}$  release. Under LY and LF sites, the and slightly lower pH under NTS (Table 1) promotes the dissolution of  $\text{CaCO}_3$  into  $\text{Ca}^{2+}$ . Meanwhile, certain rhizosphere microbes may further enhance this process by secreting organic acids (Ball et al. 2023). Overall, compared with conventional tillage, conservation tillage reduces aggregate turnover, enhances organic inputs from residues and roots, and increases the availability of key mineral components (i.e., Feo and  $\text{Ca}^{2+}$ ), thereby promoting the formation and stability of macroaggregates.

The functional group composition of SOC is a more important predictor affecting aggregate stability (Figure 6B). In this study, NTS enhanced the aromatic-C content, polysaccharide-C and aromatic-C/aliphatic-atin different sites, resulting in larger MWD. Crop straw contains many hydrophobic components, such as lignin-derived aromatic-C, which can reduce water infiltration and form hydrophobic coatings around SOC (Ndzelu et al. 2023; Saidy et al. 2012). Polysaccharide-C, derived from plant residues and microbial secretions, acts as a biological glue that promotes microaggregate formation and short-term soil structural stability, especially under conservation tillage (Tisdall and Oades 1982; Six et al. 2004). This promotes the physical protection of organic matter and contributes to the stabilization of soil aggregate structure under NTS. Moreover, in some calcareous soils and soils rich in iron oxides, the formation of organic-mineral complexes promotes soil aggregation (Li et al. 2022; Sindelar et al. 2015). In our study, exchangeable Ca and Feo indirectly promoted macroaggregate formation by

binding with SOC functional groups (Figure 6B). This chemical association can form stable organo-mineral complexes that enhance aggregate stability (Liu et al. 2023). NTS improves aggregate stability by increasing key chemical groups and their bonding with mineral ions.

Soil types with distinct physicochemical properties significantly influence the distribution and stability of soil aggregates (Figure 6A). CC (Phaeozems) with large clay contents was characterized by lower pH and temperature but a larger MWD value (Figure S1). Furthermore, we found that Phaeozems had larger Feo content, exchangeable Ca content, and a larger SSA than LY (Calcaric Cambisols) and LF (Calcic Luvisols) (Figure 4). This may enhance the interaction between mineral ions and residue inputs, promoting the formation of organo-mineral complexes that bind soil particles into larger aggregates (Andruschkewitsch et al. 2013). This process contributes to substantially greater SOC storage under Phaeozems than other sites (Figure 2). Notably, the interaction effects revealed the largest SOC increase under NTS at the LY site, while the most pronounced increases in MBC and MBN were observed at the LF site (Table 1). Furthermore, NTS led to the greatest increases in MWD and the macroaggregate-associated SOC and TN storage (29.8%) at the Calcaric Cambisols compared to Calcic Luvisols (21.3%) and Phaeozems (20.7%). As highlighted in previous studies, soils with low baseline SOC levels in certain regions tend to show a greater capacity for SOC enhancement and a stronger response to conservation tillage (Ding et al. 2006; Lal 2004). More importantly, we found that Calcaric Cambisols and Calcic Luvisols under NTS not only showed increased Feo content but also significantly larger  $\text{Ca}^{2+}$  concentrations, while  $\text{Ca}^{2+}$  levels at the Phaeozems did not differ significantly between NTS and CT treatments (Figure 4). Mineral ions, acting as inorganic binding agents, further promote aggregate formation and stabilization (Mustafa et al. 2022). Despite differing durations, all three sites exceed 10 years, and their mineralogical differences mainly reflect parent material and long-term management, as soil weathering and structural change are slow (Panettieri et al. 2020). At the LF site, the 4-year earlier sampling may affect dynamic properties (e.g., soil microbial activity and soluble ions), but SOC storage remains stable or changes only slightly after 26 years of consistent tillage management and climate (Figure S5). Our study mainly focused on mineralogical effects on SOC stability. Future work with more sites could provide further insights into the saturation of mineral surfaces with organic carbon across temporal and spatial scales. Taken together, long-term conservation tillage emerges as an effective strategy to mitigate SOC depletion and sustain agricultural productivity by enhancing both the aggregate physical protection and mineral-associated stabilization of SOC across different sites. This positive effect on aggregate stability and mineral protection is particularly notable in calcareous soils with a low carbon baseline, which exhibit strong potential for increasing carbon storage.

## 5 | Conclusion

The annual average carbon (C) sequestration rate in the 0–20 cm soil layer under NTS ranged from 0.03 to 0.103  $\text{Mg ha}^{-1} \text{ year}^{-1}$ , resulting in a 17.8%–28.3% increase in SOC storage compared to conventional tillage (CT) across Calcaric Cambisols, Calcic

Luvisols, and Phaeozems. This improvement was primarily attributed to mineral-mediated aggregate stability and carbon chemical associations. NTS promoted macroaggregate formation and increased aggregate stability, thereby improving the physical protection of SOC and TN within aggregates. In addition, NTS increased the relative proportions of aromatic-C and polysaccharide-C and elevated the aromatic-C/aliphatic-C ratio, which were positively correlated with greater levels of amorphous iron (Feo), exchangeable calcium (Ca<sup>2+</sup>), and SSA. These mineral ions, through selective binding with organic carbon functional groups, promoted soil aggregation and the formation of stable organo-mineral complexes, thereby enhancing both the physical and chemical stabilization of SOC. Among the three sites, Phaeozems showed the largest SOC storage, along with elevated Feo and Ca<sup>2+</sup> contents and a greater aromatic-C/aliphatic-C ratio. However, interaction effects indicated that the greatest increases in MWD and macroaggregate-associated SOC and TN under NTS occurred in Calcaric Cambisols, likely due to the greater enhancement of Feo and Ca<sup>2+</sup> in the soil. Overall, conservation tillage enhanced SOC storage by strengthening both chemical interactions and mineral-mediated physical protection of aggregates, making it a promising approach to mitigate carbon loss and promote sustainable agricultural development, particularly in Calcaric Cambisols with smaller initial carbon levels and more responsive mineral activity.

#### Author Contributions

**Zixuan Han:** conceptualization, writing – review and editing, writing – original draft, formal analysis. **Aurore Degré:** conceptualization. **Shengping Li:** software. **Xiaojun Song:** methodology. **Huizhou Gao:** data curation. **Angyuan Jia:** validation. **Qiqi Gao:** data curation. **Xueping Wu:** funding acquisition, supervision. **Aizhen Liang:** resources, supervision.

#### Acknowledgements

This work was financially supported by the National Key Research and Development Program of China (2023YFD1500301). The authors thank researchers at the station of Northeast Institute of Geography and Agroecology for their help maintaining the field experiments. The authors would like to express sincere gratitude to the professors from the University of Liège for their valuable suggestions and thank TopEdit ([www.topeditsci.com](http://www.topeditsci.com)) for its linguistic assistance during the preparation of this manuscript. We also thank the editors for their efforts.

#### Data Availability Statement

The data that support the findings of this study are available on request from the corresponding author. The data are not publicly available due to privacy or ethical restrictions.

#### References

Adhikari, D., and Y. Yang. 2015. “Selective Stabilization of Aliphatic Organic Carbon by Iron Oxide.” *Scientific Reports* 5: 11214. <https://doi.org/10.1038/srep11214>.

Almagro, M., A. Ruiz-Navarro, E. Díaz-Pereira, J. Albaladejo, and M. Martínez-Mena. 2021. “Plant Residue Chemical Quality Modulates the Soil Microbial Response Related to Decomposition and Soil Organic Carbon and Nitrogen Stabilization in a Rainfed Mediterranean

Agroecosystem.” *Soil Biology and Biochemistry* 156: 108198. <https://doi.org/10.1016/j.soilbio.2021.108198>.

Andruschkewitsch, R., D. Geisseler, H.-J. Koch, and B. Ludwig. 2013. “Effects of Tillage on Contents of Organic Carbon, Nitrogen, Water-Stable Aggregates and Light Fraction for Four Different Long-Term Trials.” *Geoderma* 192: 368–377. <https://doi.org/10.1016/j.geoderma.2012.07.005>.

Atere, C. T., A. Gunina, Z. Zhu, et al. 2020. “Organic Matter Stabilization in Aggregates and Density Fractions in Paddy Soil Depending on Long-Term Fertilization: Tracing of Pathways by <sup>13</sup>C Natural Abundance.” *Soil Biology and Biochemistry* 149: 107931. <https://doi.org/10.1016/j.soilbio.2020.107931>.

Bailey, V. L., J. L. Smith, and H. Bolton Jr. 2002. “Fungal-to-Bacterial Ratios in Soils Investigated for Enhanced C Sequestration.” *Soil Biology and Biochemistry* 34, no. 7: 997–1007. [https://doi.org/10.1016/S0038-0717\(02\)00033-0](https://doi.org/10.1016/S0038-0717(02)00033-0).

Ball, K. R., A. A. Malik, C. Muscarella, and J. C. Blankinship. 2023. “Irrigation Alters Biogeochemical Processes to Increase Both Inorganic and Organic Carbon in Arid-Calcic Cropland Soils.” *Soil Biology and Biochemistry* 187: 109189. <https://doi.org/10.1016/j.soilbio.2023.109189>.

Barberis, E., F. Ajmone Marsan, V. Boero, and E. Arduino. 1991. “Aggregation of Soil Particles by Iron Oxides in Various Size Fractions of Soil B Horizons.” *European Journal of Soil Science* 42, no. 4: 535–542. <https://doi.org/10.1111/j.1365-2389.1991.tb00100.x>.

Cai, Y., T. Ma, Y. Wang, et al. 2022. “Assessing the Accumulation Efficiency of Various Microbial Carbon Components in Soils of Different Minerals.” *Geoderma* 407: 115562. <https://doi.org/10.1016/j.geoderma.2021.115562>.

Cotrufo, M. F., J. L. Soong, A. J. Horton, et al. 2015. “Formation of Soil Organic Matter via Biochemical and Physical Pathways of Litter Mass Loss.” *Nature Geoscience* 8: 776–779. <https://doi.org/10.1038/ngeo2520>.

Cotrufo, M. F., M. D. Wallenstein, C. M. Boot, K. Denef, and E. Paul. 2013. “The Microbial Efficiency-Matrix Stabilization (MEMS) Framework Integrates Plant Litter Decomposition With Soil Organic Matter Stabilization: Do Labile Plant Inputs Form Stable Soil Organic Matter?” *Global Change Biology* 19: 988–995. <https://doi.org/10.1111/gcb.12113>.

Ding, W., Y. Zhang, B. Zhu, and X. Yang. 2006. “Soil Carbon Sequestration Potential of Agricultural Soils in China Under Different Tillage and Residue Management Practices.” *Soil and Tillage Research* 90: 61–71. <https://doi.org/10.1016/j.still.2005.08.014>.

Dorodnikov, M., E. Blagodatskaya, S. Blagodatsky, S. Marhan, A. Fangmeier, and Y. Kuzyakov. 2009. “Stimulation of Microbial Extracellular Enzyme Activities by Elevated CO<sub>2</sub> Depends on Soil Aggregate Size.” *Global Change Biology* 15: 1603–1614. <https://doi.org/10.1111/j.1365-2486.2009.01844.x>.

Dou, X., J. Zhang, C. Zhang, et al. 2023. “Calcium Carbonate Regulates Soil Organic Carbon Accumulation by Mediating Microbial Communities in Northern China.” *Catena* 231: 107327. <https://doi.org/10.1016/j.catena.2023.107327>.

Engell, I., D. Linsler, M. Sandor, R. G. Joergensen, C. Meinen, and M. Potthoff. 2022. “The Effects of Conservation Tillage on Chemical and Microbial Soil Parameters at Four Sites Across Europe.” *Plants* 11: 1747. <https://doi.org/10.3390/plants11131747>.

Gao, L., E. Becker, G. Liang, et al. 2017. “Effect of Different Tillage Systems on Aggregate Structure and Inner Distribution of Organic Carbon.” *Geoderma* 288: 97–104. <https://doi.org/10.1016/j.geoderma.2016.11.005>.

Gao, L., B. Wang, S. Li, et al. 2019. “Effects of Different Long-Term Tillage Systems on the Composition of Organic Matter by <sup>13</sup>C CP/TOSS NMR in Physical Fractions in the Loess Plateau of China.” *Soil and Tillage Research* 194: 104321. <https://doi.org/10.1016/j.still.2019.104321>.



- Gao, Y., H. Feng, M. Zhang, et al. 2023. "Straw Returning Combined With Controlled-Release Nitrogen Fertilizer Affected Organic Carbon Storage and Crop Yield by Changing Humic Acid Composition and Aggregate Distribution." *Journal of Cleaner Production* 415: 137783. <https://doi.org/10.1016/j.jclepro.2023.137783>.
- Guan, D., Y. Zhang, M. M. Al-Kaisi, Q. Wang, M. Zhang, and Z. Li. 2015. "Tillage Practices Effect on Root Distribution and Water Use Efficiency of Winter Wheat Under Rain-Fed Condition in the North China Plain." *Soil and Tillage Research* 146: 286–295. <https://doi.org/10.1016/j.still.2014.09.016>.
- Hao, X., X. Han, S. Wang, and L. J. Li. 2022. "Dynamics and Composition of Soil Organic Carbon in Response to 15 Years of Straw Return in a Mollisol." *Soil and Tillage Research* 215: 105221. <https://doi.org/10.1016/j.still.2021.105221>.
- Hartmann, M., and J. Six. 2023. "Soil Structure and Microbiome Functions in Agroecosystems." *Nature Reviews Earth and Environment* 4: 4–18. <https://doi.org/10.1038/s43017-022-00366-w>.
- Hood-Nowotny, R., N. H.-N. Umana, E. Inselbacher, P. Oswald-Lachouani, and W. Wanek. 2010. "Alternative Methods for Measuring Inorganic, Organic, and Total Dissolved Nitrogen in Soil." *Soil Science Society of America Journal* 74: 1018–1027. <https://doi.org/10.2136/sssaj.2009.0389>.
- Houba, V. J. G., E. J. M. Temminghoff, G. A. Gaikhorst, and W. van Vark. 2000. "Soil Analysis Procedures Using 0.01 M Calcium Chloride as Extraction Reagent." *Communications in Soil Science and Plant Analysis* 31, no. 9–10: 1299–1396. <https://doi.org/10.1080/00103620009370514>.
- Inda, A. V., J. Torrent, V. Barrón, C. Bayer, and J. R. Fink. 2013. "Iron Oxides Dynamics in a Subtropical Brazilian Paleudult Under Long-Term No-Tillage Management." *Scientia Agricola* 70: 48–54. <https://doi.org/10.1590/S0103-90162013000100008>.
- Jat, H. S., A. Datta, M. Choudhary, et al. 2019. "Effects of Tillage, Crop Establishment and Diversification on Soil Organic Carbon, Aggregation, Aggregate Associated Carbon and Productivity in Cereal Systems of Semi-Arid Northwest India." *Soil and Tillage Research* 190: 128–138. <https://doi.org/10.1016/j.still.2019.03.005>.
- Kan, Z. R., W. X. Liu, W. S. Liu, et al. 2022. "Mechanisms of Soil Organic Carbon Stability and Its Response to No-Till: A Global Synthesis and Perspective." *Global Change Biology* 28: 693–710. <https://doi.org/10.1111/gcb.15968>.
- Kan, Z. R., S. T. Ma, Q. Y. Liu, et al. 2020. "Carbon Sequestration and Mineralization in Soil Aggregates Under Long-Term Conservation Tillage in the North China Plain." *Catena* 188: 104428. <https://doi.org/10.1016/j.catena.2019.104428>.
- Karlen, D. L., J. L. Kovar, C. A. Cambardella, and T. S. Colvin. 2013. "Thirty-Year Tillage Effects on Crop Yield and Soil Fertility Indicators." *Soil and Tillage Research* 130: 24–41. <https://doi.org/10.1016/j.still.2013.02.003>.
- Kemper, W. D., and R. C. Rosenau. 1986. "Aggregate Stability and Size Distribution." In *Methods of Soil Analysis. Part 1*, edited by A. Klute, 2nd ed., 425–442. American Society of Agronomy and Soil Science Society of America.
- Kirsten, M., R. Mikutta, C. Vogel, et al. 2021. "Iron Oxides and Aluminous Clays Selectively Control Soil Carbon Storage and Stability in the Humid Tropics." *Scientific Reports* 11: 5076. <https://doi.org/10.1038/s41598-021-84777-7>.
- Kögel-Knabner, I. 2017. "The Macromolecular Organic Composition of Plant and Microbial Residues as Inputs to Soil Organic Matter: Fourteen Years On." *Soil Biology and Biochemistry* 105: A3–A8. <https://doi.org/10.1016/j.soilbio.2016.08.011>.
- Lal, R. 2004. "Soil Carbon Sequestration Impacts on Global Climate Change and Food Security." *Science* 304: 1623–1627. <https://doi.org/10.1126/science.1097396>.
- Lee, J., J. W. Hopmans, D. E. Rolston, S. G. Baer, and J. Six. 2009. "Determining Soil Carbon Stock Changes: Simple Bulk Density Corrections Fail." *Agriculture, Ecosystems and Environment* 134: 251–256. <https://doi.org/10.1016/j.agee.2009.07.006>.
- Li, Y., Z. Chen, J. Chen, et al. 2022. "Oxygen Availability Regulates the Quality of Soil Dissolved Organic Matter by Mediating Microbial Metabolism and Iron Oxidation." *Global Change Biology* 28: 7410–7427. <https://doi.org/10.1111/gcb.16445>.
- Liang, C., J. P. Schimel, and J. D. Jastrow. 2019. "The Importance of Anabolism in Microbial Control Over Soil Carbon Storage." *Nature Microbiology* 4: 684–690. <https://doi.org/10.1038/s41564-019-0363-6>.
- Liang, Y., M. Al-Kaisi, J. Yuan, et al. 2021. "Effect of Chemical Fertilizer and Straw-Derived Organic Amendments on Continuous Maize Yield, Soil Carbon Sequestration and Soil Quality in a Chinese Mollisol." *Agriculture, Ecosystems and Environment* 314: 107403. <https://doi.org/10.1016/j.agee.2021.107403>.
- Liu, L., A. Gunina, F. Zhang, Z. Cui, and J. Tian. 2023. "Fungal Necromass Increases Soil Aggregation and Organic Matter Chemical Stability Under Improved Cropland Management and Natural Restoration." *Science of the Total Environment* 858: 159953. <https://doi.org/10.1016/j.scitotenv.2022.159953>.
- Maltoni, K. L., L. M. M. De Mello, and W. E. Dubbin. 2017. "The Effect of Ferral Soil Mineralogy on the Distribution of Organic C Across Aggregate Size Fractions Under Native Vegetation and No-Tillage Agriculture." *Soil Use and Management* 33: 328–338. <https://doi.org/10.1111/sum.12339>.
- Margenot, A. J., S. J. Parikh, and F. J. Calderón. 2023. "Fourier-Transform Infrared Spectroscopy for Soil Organic Matter Analysis." *Soil Science Society of America Journal* 87, no. 6: 1503–1528. <https://doi.org/10.1002/saj2.20583>.
- McLean, E. O. 1982. "Soil pH and Lime Requirement." *Soil Science Society of America Journal* 46, no. 6: 1276–1281. <https://doi.org/10.2136/sssaj1982.03615995004600060020x>.
- Mustafa, A., J. Frouz, M. Naveed, et al. 2022. "Stability of Soil Organic Carbon Under Long-Term Fertilization: Results From <sup>13</sup>C NMR Analysis and Laboratory Incubation." *Environmental Research* 205: 112476. <https://doi.org/10.1016/j.envres.2021.112476>.
- Muukkonen, P., H. Hartikainen, K. Lahti, A. Särkelä, M. Puustinen, and L. Alakukku. 2007. "Influence of No-Tillage on the Distribution and Lability of Phosphorus in Finnish Clay Soils." *Agriculture, Ecosystems and Environment* 120: 299–306. <https://doi.org/10.1016/j.agee.2006.09.012>.
- Nandan, R., V. Singh, S. S. Singh, et al. 2019. "Impact of Conservation Tillage in Rice-Based Cropping Systems on Soil Aggregation, Carbon Pools and Nutrients." *Geoderma* 340: 104–114. <https://doi.org/10.1016/j.geoderma.2019.01.001>.
- Ndzelu, B. S., S. Dou, X. Zhang, and Y. Zhang. 2023. "Molecular Composition and Structure of Organic Matter in Density Fractions of Soils Amended With Corn Straw for Five Years." *Pedosphere* 33: 372–380. <https://doi.org/10.1016/j.pedsph.2022.06.057>.
- Nyamadzawo, G., J. Nyamangara, P. Nyamugafata, and A. Muzulu. 2009. "Soil Microbial Biomass and Mineralization of Aggregate Protected Carbon in Fallow-Maize Systems Under Conventional and No-Tillage in Central Zimbabwe." *Soil and Tillage Research* 102: 151–157. <https://doi.org/10.1016/j.still.2008.08.007>.
- Panettieri, M., L. L. de Sosa, M. T. Domínguez, and E. Madejón. 2020. "Long-Term Impacts of Conservation Tillage on Mediterranean Agricultural Soils: Shifts in Microbial Communities Despite Limited Effects on Chemical Properties." *Agriculture, Ecosystems and Environment* 304: 107144. <https://doi.org/10.1016/j.agee.2020.107144>.
- Panettieri, M., H. Knicker, J. M. Murillo, E. Madejón, and P. G. Hatcher. 2014. "Soil Organic Matter Degradation in an Agricultural Chronosequence Under Different Tillage Regimes Evaluated by



- Organic Matter Pools, Enzymatic Activities and CPMAS  $^{13}\text{C}$  NMR." *Soil Biology and Biochemistry* 78: 170–181. <https://doi.org/10.1016/j.soilbio.2014.07.021>.
- Plaza, C., D. Courtier-Murias, J. M. Fernández, A. Polo, and A. J. Simpson. 2013. "Physical, Chemical, and Biochemical Mechanisms of Soil Organic Matter Stabilization Under Conservation Tillage Systems: A Central Role for Microbes and Microbial By-Products in C Sequestration." *Soil Biology and Biochemistry* 57: 124–134. <https://doi.org/10.1016/j.soilbio.2012.07.026>.
- Saidy, A. R., R. J. Smernik, J. A. Baldock, K. Kaiser, J. Sanderman, and L. M. Macdonald. 2012. "Effects of Clay Mineralogy and Hydrous Iron Oxides on Labile Organic Carbon Stabilization." *Geoderma* 173: 104–110. <https://doi.org/10.1016/j.geoderma.2011.12.030>.
- Sarker, J. R., B. P. Singh, A. L. Cowie, et al. 2018. "Carbon and Nutrient Mineralisation Dynamics in Aggregate-Size Classes From Different Tillage Systems After Input of Canola and Wheat Residues." *Soil Biology and Biochemistry* 116: 22–38. <https://doi.org/10.1016/j.soilbio.2017.09.030>.
- Schweizer, S. A., F. B. Bucka, M. Graf-Rosenfellner, and I. Kögel-Knabner. 2019. "Soil Microaggregate Size Composition and Organic Matter Distribution as Affected by Clay Content." *Geoderma* 355: 113901. <https://doi.org/10.1016/j.geoderma.2019.113901>.
- Shabtai, I. A., R. C. Wilhelm, S. A. Schweizer, C. Höschen, D. H. Buckley, and J. Lehmann. 2023. "Calcium Promotes Persistent Soil Organic Matter by Altering Microbial Transformation of Plant Litter." *Nature Communications* 14: 6609. <https://doi.org/10.1038/s41467-023-42291-6>.
- Sindelar, H. R., M. T. Brown, and T. H. Boyer. 2015. "Effects of Natural Organic Matter on Calcium and Phosphorus Co-Precipitation." *Chemosphere* 138: 218–224. <https://doi.org/10.1016/j.chemosphere.2015.05.008>.
- Six, J., H. Bossuyt, S. Degryze, and K. Denef. 2004. "A History of Research on the Link Between (Micro)aggregates, Soil Biota, and Soil Organic Matter Dynamics." *Soil and Tillage Research* 79, no. 1: 7–31. <https://doi.org/10.1016/j.still.2004.03.008>.
- Soong, J. L., F. J. Calderón, J. M. Betzen, and M. F. Cotrufo. 2014. "Quantification and FTIR Characterization of Dissolved Organic Carbon and Total Dissolved Nitrogen Leached From Litter: A Comparison of Methods Across Litter Types." *Plant and Soil* 385: 125–137. <https://doi.org/10.1007/s11040-014-2232-4>.
- Sowers, T. D., D. Adhikari, J. Wang, Y. Yang, and D. L. Sparks. 2018. "Spatial Associations and Chemical Composition of Organic Carbon Sequestered in Fe, Ca, and Organic Carbon Ternary Systems." *Environmental Science and Technology* 52: 6936–6944. <https://doi.org/10.1021/acs.est.8b01158>.
- Spaccini, R., A. Piccolo, G. Haberhauer, and M. H. Gerzabek. 2000. "Transformation of Organic Matter From Maize Residues Into Labile and Humic Fractions of Three European Soils as Revealed by  $^{13}\text{C}$  CPMAS NMR Spectroscopy." *European Journal of Soil Science* 51, no. 2: 219–230. <https://doi.org/10.1046/j.1365-2389.2000.00305.x>.
- Speiser, J. L., M. E. Miller, J. Tooze, and E. Ip. 2019. "A Comparison of Random Forest Variable Selection Methods for Classification Prediction Modeling." *Expert Systems With Applications* 134: 93–101. <https://doi.org/10.1016/j.eswa.2019.05.028>.
- Szymański, W. 2017. "Chemistry and Spectroscopic Properties of Surface Horizons of Arctic Soils Under Different Types of Tundra Vegetation: A Case Study From the Fuglebergsletta Coastal Plain (SW Spitsbergen)." *Catena* 156: 325–337. <https://doi.org/10.1016/j.catena.2017.04.024>.
- Tisdall, J. M., and J. M. Oades. 1982. "Organic Matter and Water-Stable Aggregates in Soils." *Journal of Soil Science* 33, no. 2: 141–163. <https://doi.org/10.1111/j.1365-2389.1982.tb01755.x>.
- Tivet, F., J. C. de Moraes Sá, R. Lal, et al. 2013. "Aggregate C Depletion by Plowing and Its Restoration by Diverse Biomass-C Inputs Under No-Till in Sub-Tropical and Tropical Regions of Brazil." *Soil and Tillage Research* 126: 203–218. <https://doi.org/10.1016/j.still.2012.09.004>.
- Urbanek, E., P. Hallett, D. Feeney, and R. Horn. 2007. "Water Repellency and Distribution of Hydrophilic and Hydrophobic Compounds in Soil Aggregates From Different Tillage Systems." *Geoderma* 140: 147–155. <https://doi.org/10.1016/j.geoderma.2007.04.001>.
- Wan, D., M. Ma, N. Peng, et al. 2021. "Effects of Long-Term Fertilization on Calcium-Associated Soil Organic Carbon: Implications for C Sequestration in Agricultural Soils." *Science of the Total Environment* 772: 145037. <https://doi.org/10.1016/j.scitotenv.2021.145037>.
- Wang, W., J. Yuan, S. Gao, et al. 2020. "Conservation Tillage Enhances Crop Productivity and Decreases Soil Nitrogen Losses in a Rainfed Agroecosystem of the Loess Plateau, China." *Journal of Cleaner Production* 274: 122854. <https://doi.org/10.1016/j.jclepro.2020.122854>.
- Wendt, J. W., and S. Hauser. 2013. "An Equivalent Soil Mass Procedure for Monitoring Soil Organic Carbon in Multiple Soil Layers." *European Journal of Soil Science* 64, no. 1: 58–65. <https://doi.org/10.1111/ejss.12002>.
- Witzgall, K., A. Vidal, D. I. Schubert, et al. 2021. "Particulate Organic Matter as a Functional Soil Component for Persistent Soil Organic Carbon." *Nature Communications* 12. <https://doi.org/10.1038/s41467-021-24192-8>.
- World reference base for soil resources 2014. 2015. *International Soil Classification System for Naming Soils and Creating Legends for Soil Maps*. FAO.
- Xiao, K.-Q., Y. Zhao, C. Liang, et al. 2023. "Introducing the Soil Mineral Carbon Pump." *Nature Reviews Earth and Environment* 4: 135–136. <https://doi.org/10.1038/s43017-023-00396-y>.
- Xue, B., L. Huang, Y. Huang, Z. Yin, X. Li, and J. Lu. 2019. "Effects of Organic Carbon and Iron Oxides on Soil Aggregate Stability Under Different Tillage Systems in a Rice–Rape Cropping System." *Catena* 177: 1–12. <https://doi.org/10.1016/j.catena.2019.01.035>.
- Zhang, M., S. Li, X. Wu, et al. 2022. "Nitrogen Addition Mediates the Effect of Soil Microbial Diversity on Microbial Carbon Use Efficiency Under Long-Term Tillage Practices." *Land Degradation and Development* 33: 2258–2275. <https://doi.org/10.1002/ldr.4279>.
- Zhang, S., Q. Li, X. Zhang, K. Wei, L. Chen, and W. Liang. 2012. "Effects of Conservation Tillage on Soil Aggregation and Aggregate Binding Agents in Black Soil of Northeast China." *Soil and Tillage Research* 124: 196–202. <https://doi.org/10.1016/j.still.2012.06.007>.
- Zhou, M., Y. Xiao, X. Zhang, et al. 2022. "Fifteen Years of Conservation Tillage Increases Soil Aggregate Stability by Altering the Contents and Chemical Composition of Organic Carbon Fractions in Mollisols." *Land Degradation and Development* 33: 2932–2944. <https://doi.org/10.1002/ldr.4365>.

## Supporting Information

Additional supporting information can be found online in the Supporting Information section. **Table S1:** The initial soil physical and chemical properties at different locations. **Figure S1:** The percentage of different aggregate size classes and mean weight diameter (MWD) at 0–20 cm soil depth under conventional tillage (plow tillage with straw removal, CT) and no tillage with straw return (NTS) at three different sites. Different lowercase letters indicate significant difference between three sites ( $p < 0.05$ ). Asterisks indicate significant differences between NTS and CT ( $*p < 0.05$ ,  $**p < 0.01$ ,  $***p < 0.001$ ). **Figure S2:** Pearson correlation analysis between soil physico-chemical properties and crop yield of different sites and tillage practices. AVN, available nitrogen; AVP, available phosphorus; BD, bulk density; LMac, large macroaggregates ( $> 2\text{ mm}$ ); MBC, microbial biomass carbon; MBN, microbial biomass nitrogen; Mic, microaggregates ( $< 2\text{ mm}$ ); SMac, small macroaggregates ( $0.25\text{--}2\text{ mm}$ ); SOC, soil organic carbon; TN, total nitrogen. Asterisks indicate significant differences between different indicators

(\* $p < 0.05$ , \*\* $p < 0.01$ , \*\*\* $p < 0.001$ ). **Figure S3:** The Fourier-transform infrared spectra under conventional tillage (plow tillage with straw removal, CT) and no tillage with straw return (NTS) of bulk soil and aggregates at three different sites. Different lowercase letters indicate significant difference between three sites ( $p < 0.05$ ). Asterisks indicate significant differences between NTS and CT (\* $p < 0.05$ , \*\* $p < 0.01$ , \*\*\* $p < 0.001$ ). **Figure S4:** The crop yield under conventional tillage (plow tillage with straw removal, CT) and no tillage with straw return (NTS) at three different sites. Different lowercase letters indicate significant difference between three sites ( $p < 0.05$ ). Asterisks indicate significant differences between NTS and CT (\* $p < 0.05$ , \*\* $p < 0.01$ , \*\*\* $p < 0.001$ ). **Figure S5:** Monthly average temperature and precipitation at the LF site from August 2017 to September 2021.